Study of a Cooling Device of Confined Impacting Air Jets on a Heating Cylinder

Nicolas Chauchat, Éric Schall, M. Mory, M. de La Llave Plata, V.G. Couaillier

Study of a cooling device of confined impacting air jets on a heating cylinder

Nicolas Chauchat [1], Eric Schall [2], Mathieu Mory [3], Marta de la Llave Plata [4], Vincent Couaillier [5]

[1] IPRA-SIAME – UFR Sciences et techniques de Pau – Avenue de l'Université, 64013 Pau, France, nicolas.chauchat@univ-pau.fr

[2] Corresponding author, IPRA-SIAME – UFR Sciences et techniques de Pau – Avenue de l'Université, 64013 Pau, France, eric.schall@univ-pau.fr

[3] Université de Pau et des Pays de l'Adour, ENSGTI-SIAME, rue Jules Ferry, BP 7511, 64075 PAU Cedex, France, mathieu.mory@univ-pau.fr

[4] ONERA – The French Aerospace Lab – 29 avenue de la Division Leclerc, 92332 Châtillon, France, marta.de_la_llave_plata@onera.fr

[5] ONERA – The French Aerospace Lab – 29 avenue de la Division Leclerc, 92332 Châtillon, France, vincent.couaillier@onera.fr

ABSTRACT

Future aircraft technology will increasingly rely on electrical power. The substitution of mechanical energy by electrical energy will lead to an increasing amount of heat power that has to be evacuated. Thus innovative cooling processes have to be set up according to constraints imposed by the technological design. The present study is conducted within the framework of onboard aircraft. We aim at studying a new cooling system of a small turbo engine stator. The cooling techniques, fully designed and built at Pau University, consists in air jets impacting around a heated circular cylinder. As the inlet velocity magnitude given by the experience is relatively low (V_{in}=4,37m/s - Mach$_{in}$=0.0125), the use of a compressible solver presents a number of difficulties. In this paper we study the performance of two different compressible solvers, one based on the finite volume approach, and the other on a discontinuous Galerkin method, as well as of an incompressible solver, for this low Mach number configuration. Some of the numerical results are compared to the available experimental data.

1. INTRODUCTION AND CONTEXT

"Green aircraft projects" aim at reducing greenhouse gas emissions, pollutants and fuel consumption. It seems that aircraft electrical systems are growing in all aeronautical programs for many reasons. Indeed, the "All-Electric E-Fan 2.0 Airplane" project by Airbus and the Boeing "Subsonic Ultra-Green Aircraft Research" (SUGAR) program investigate technologies that might allow the subsonic commercial aircrafts to meet environmental requirements in 2030 to 2050. Recent research like GREENAIR (7th RTD European framework programme) or the recent technological achievements on the A380 as on the Boeing 787 demonstrates that the use of electricity is increasing on-board. The use of electrical energy instead of mechanical energy is a challenge for aircraft equipment manufacturers. However, electrical processes lead to an additional thermal charge that needs to be evacuated. Thus, dedicated new cooling system devices have to be developed. Up to now, for some industrial applications, using air flow remains one of the best solutions for cooling electrical machines, while satisfying the objective of lower cost and weight.

This project has been awarded a grant coming from the DGCIS* research funds (France) for four years after getting the label from the three French aeronautical hubs. The original studied device can represent any small turbo-engine and have a huge potential for industrial applications not only restricted to the aeronautic sector. The implemented new cooling process is based on four normal (or radial) air jet impacts on a heating cylinder (see Fig. 1). The cooling air is injected through four radial slots respectively oriented north, south, east and west. The confined fluid leaves the cylinder through four others radial slots shifted 45 degrees from the inlets. Taking as reference the set of experimental data obtained by setting the inlet velocity to 4,37m/s via a flowmeter, we have launched a series of CFD simulations

using three different numerical methods. Two compressible solvers have been considered, the **elsA** solver based on a finite volume approach, and the Aghora solver based on a discontinuous Galerkin method, as well as an incompressible solver of ANSYS-Fluent. Indeed even if the inlet Mach number is relatively low ($Mach_{in}=0.0125$) the authors are not convinced that the fluid is devoid of any compressibility effect. It is well known that the numerical resolution of the compressible set of the Navier-Stokes equations at very low Mach numbers is very sensitive to numerical errors, specially when low-order discretizations are considered. Here we compare the results provided by **elsA** and Aghora for which the spatial order of accuracy is set to second order. In the case of the Aghora solver this implies setting the polynomial degree to 1 (p=1). However, we should note that the DG method will ensure that the formal order of accuracy is 2 on irregular meshes, as opposed to the finite volume approach for which the order of accuracy is not preserved in the case of irregular meshes. The authors hope that this 3-ways numerical computation with the experiment will help them in the understanding on the low compressibility effects. To this end, two different levels of comparisons are considered, the coarse level and the particle level (which is the finest of the two). At the coarse level, comparisons will be performed on the global transported convective heat flux transported and the mass balance in the cavity. At the particle level, we look into the inner wall heat flux in the azimuthal direction as well as the pattern of streamlines inside the cavity.

This paper is organised as follows. The original set-up is described in section 2. A presentation of the numerical methods used in the three softwares considered in this research is provided in section 3. At the end of sections 2 and 3, a brief discussion attempts to emphasize the inherent difficulties linked to the experiment and the CFD simulations. In section 4, the results from the comparisons between the different simulations and the experiment are discussed. Finally in the last section we summarize some of the main difficulties in CFD about the compressibility assumption linked with moving fluid inside complex geometries. The nature of the perspectives gives some of the very big challenges expecting in such a low-Mach numerical simulations for future.

2. EXPERIMENTAL DESIGN

The experimental set-up achieves the cooling of the surface of a circular cylinder (radius $R_i=5.4cm$) by 4 plane jets impacting perpendicularly the heated cylinder. As shown in Fig. 1, the four impacting jets are directed from the north, east, south and west, respectively. The heated air is extracted through four outlet slots, the directions of which are along the angle bisector between neighbouring inlet jets. The flow is confined in the annular domain with internal radius R_i and external radius $R_f=7cm$. The slot width is $S_f=3.6mm$. Numerical simulations were carried out assuming 2D flow, i.e. it does vary in the direction Oz perpendicular to the cross-section shown in Fig. 1. The cylinder length is L=4.7cm in the experiment.

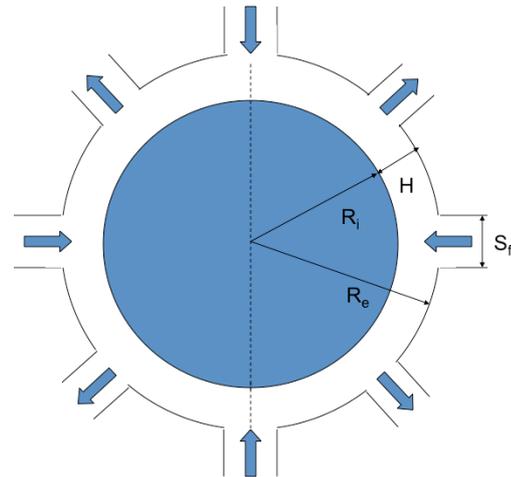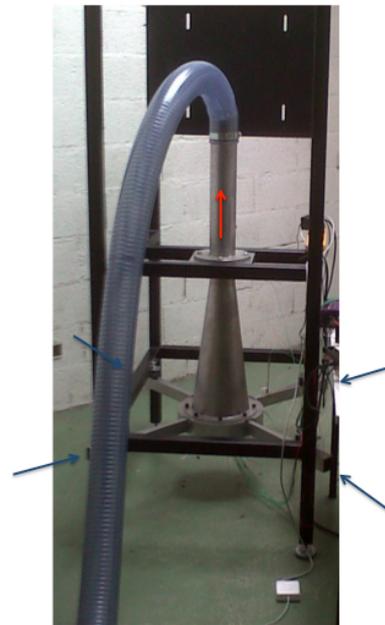*Figure 1. Cross-section of the cavity in which the flow cools the heated cylinder of radius Ri.*

2a

Figure 2. Photographs of the experimental set-up.

The photograph in Fig. 2a shows the experimental set-up. The blue arrows indicate the flow into four rectangular tubes leading to the entrance slots into the cavity. The casing ensuring the inlet distribution of the jets impacting the cylinder and collecting the warm air outside the flow cavity is shown in Fig. 2b. The heated cylinder is inserted under the cone seen in Fig. 2b, which channels the exit warm air into the vertical tube seen in Fig. 2a. The red arrow indicates the direction of the outlet flow into a flexible tube, which is downstream connected to a mass flowmeter (Eldridge 9700MPNH), a fan and a vane.

The circular cylinder is heated using an electrical resistance inserted inside an adhesive polyamide mat glued over the inner surface of the cylinder (brown in Fig. 3a). The surface temperature on the cylinder is measured using thermocouples (type K). The thermocouples wires (green in Fig. 3a) traverse the mat and the cylinder (thickness 2mm) and the measuring extremities are bended after coming up to the cylinder surface. The entire surface of the cylinder is finally wrapped by an adhesive film (supporting high temperature), which maintains the thermocouples in contact with the cylinder. Fig. 3b shows an external view of the cylinder. The locations of the thermocouples measurement are shown. The sketch at the bottom indicates that thermocouples 8, 9 and 12 are along the axis line of an impacting jet, whereas thermocouples 1, 10 and 11 are along the axis line of an outlet slot. The experimental conditions given by the mass flow rate and the electrical power P_{elec} results in a steady regime for the temperature level at the surface of the cylinder, which corresponds to the equilibrium of the furnished electrical power with the convective power extracted by the air and the conductive power transmitted through the aluminium casing.

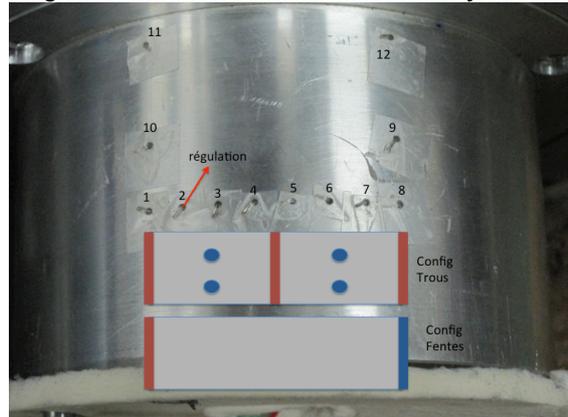*Figure 3a. Inside view of the heated cylinder.*

Figure 3b. Outside surface view of the heated cylinder showing the thermocouple positions.

The present paper focuses on a flow configuration at a Reynolds numbers lower than 1100. For the experiments considered in this paper, the electrical power delivered was reduced to 212W as compared to the maximum electrical power (420W) in order to maintain the surface temperature less than 100°C (maximum temperature supported by the resistance polyamide mat). The electrical power delivered was measured using a wattmeter. The convective thermal power extracted by the air flow was estimated from the temperature difference measured by two thermocouples (type K), one being placed inside one of the inlet tube (T_i) and the other (T_e) at the exit of an outlet slot from the cavity. Estimating the thermal convective power, $P_{conv} = c_p m (T_e - T_i)$, relies also on an accurate measurement of the mass flow rate of air m. The average surface temperature T_{surf} was finally determined from thermocouple measurements on the cylinder surface.

The present paper mainly addresses the ability of different numerical models to determine the heat transfer, for moderate Reynolds number conditions. We therefore basically compare, for a moderate Reynolds number, the couple of values of the convective thermal power P_{conv} and of the

temperature difference $T_{surf}-T_i$, obtained from the different numerical simulations with the experimental values.

Difficulties inherent in experience:
Because of its confinement, the experimental set-up does not provide access to detailed flow and thermal properties such as the flow line maps obtained from numerical or the temperature variations all over the heated cylinder. Local measurements of temperature at the surface of the heated cylinder nevertheless show limited variations of temperature at the surface of the heated cylinder, indicating that a condition of uniform parietal temperature of the cylinder is relevant. The temperature boundary conditions are fixed for the CFD computations using the experimental temperature data and the inlet flow velocity is determined from the mass flow rate measurement. The experiment also delivers the global convective power that is compared to the total convective power computed by the CFD simulations. The laboratory experiment intervene in this study through the statement of boundary conditions for CFD computations and through the comparison between experiment and simulation of the global convective transfer achieved.

3. NUMERICAL METHODS AND SOFTWARES
CFD in engineering needs broad knowledge in various disciplines like in applied mathematics, physics and programming (for those who used to practice) in the hope for careful interpretation of the numerical solutions. When one wishes to make a CFD of a physical problematic the first step consist of fixing the modeling via the determination of a set of partial differential equations (PDE). This is a very challenging step because the transition from the continuous form of the PDE to the discretized form depends also on its nature. In this work we want to see differences between both possible assumptions on the fluid, which are incompressible and compressible.

Incompressible simulation via ANSYS-Fluent:
Many authors have developed numerical methods for incompressible flows in aeronautic since the beginning of the first computer. Thanks to its long experience the authors have chosen the ANSYS-FLUENT software for computing the fluid motion inside our annular cavity. Historically the ANSYS-FLUENT software [1] has extensive experience in CFD for a wide range of flow regimes (even for compressible flows). Here, density is considered as constant via the zero-divergence of the velocity and the pressure-based method has been selected. So the unknown vector is reduced to

(P, V, T), which can be determined with the three conservation equations of the mass, the momentum and the energy. Remember that with such incompressible assumption the relation of perfect gas is not useful as the pressure is only velocity dependent. One uses to talk about the pressure-velocity coupling while the temperature is deduced from the conservation equation of the energy written in temperature and resolved alongside the others. Indeed, the employed method is segregated leading to regular corrections of the pressure along the iterative process. As the "steady" option is selected there is no time-marching in the calculation procedure. The SIMPLE and PISO algorithms have been both tested.

Compressible simulation via *elsA* and Aghora:
The *elsA* [2] software is a multi-application CFD simulation platform especially dealing with internal and external aerodynamics from the low subsonic to the high supersonic flow regime. *elsA* is the reference ONERA aerodynamics solver (see [2] and <http://elsa.onera.fr> for a exhaustive review of accomplishments both from research and industry) based on finite volume (FV) schemes for multi-bloc structured and unstructured meshes [3]. The numerical resolution can be done with different approximate Rieman solvers based on upwind and centered schemes. The solvers of Roe [4] and Jameson [5] have been chosen for this work. Note that in the case of Jameson, the chosen artificial dissipative terms are: $k^{(2)}=1$ and $k^{(4)}=0,032$.
Motivated by the fact that the demand for very accurate CFD predictions at an ever-increasing level of detail is the driving force for the development of highly accurate simulation techniques able to predict not only overall flow features, but also local values of the quantities of interest, ONERA has started the development of a solver called Aghora based on high-order space time variational methods on unstructured polyhedral elements, and mainly Discontinuous Galerkin type methods [6, 7]. A number of finite volume schemes (Lax-Friedrichs, Roe, etc.) are available to approximate the convective fluxes across the element interfaces. The viscous fluxes can be discretized by using the BR2 scheme [8] or the Symmetric Interior Penalty (SIP) method [9].

Difficulties inherent in CFD :
For a given continuous modeling via a PDE-type set this is already a challenging task to built the numerical simulation of the discrete form with the objective to reproduce the analytical solution with as accuracy as possible provided that such a

solution exists. Here two identified gaps have to be addressed. The first one concerns the right modeling choice about the fluid compressibility. The authors decided to carry out them both aware of the huge number of various scientist works done in each of the areas. So this study is far from exhaustive.

From the experience, the boundary conditions for FLUENT and **elsA** computations are given in Tab. 1.

The different options selected for the CFD with FLUENT and **elsA** appear in Tab. 2

Table 1. Physical boundary conditions.

Inlet, outlet and walls	
Density	1.2 kg.m^{-3}
Pressure	104 184.83 Pa
Inlet Temperature	302.45 K
Velocity magnitude	4.37 m.s^{-1}
Temperature - inner/heated wall	370.65 K
Temperature - external wall	342.45 K
Temperature - side walls (z=-0.0235m and z=0.0235m)	Linear between 342.45K and 370.65K

Table 2. Selected options with FLUENT and elsA.

	FLUENT (See FLUENT user's guide for more details)	elsA (See the User's reference manual of **elsA** for more details)
Inlet	Massflow_inlet Normal of inlets=(0, -1, 0) or (-1, 0, 0) mass flux=5.24 kg.m^{-2}.s^{-1}	Injmfr1 Normal of inlets=(0, -1, 0) or (-1, 0, 0) Surface mass flow=5.24 kg.m^{-2}.s^{-1} Stagnation enthalpy=303 872.42 m^2.s^{-2}
Outlet	Pressure_outlet	Outpres
Internal wall (heated wall)	wall	wallisoth
External wall	wall	wallisoth

4. RESULTS

2D-3D comparisons with elsA+Jameson

As the height (*z* direction) of the cylindrical cavity (L=4.7cm) under study is of the same order of magnitude as the medium radius (7cm), 2D and 3D computations have been carried out. Starting from the 2D mesh plan (11 628 cells in (*x,y*)), 60 other planes have been extruded to give the 3D mesh composed of 726388 (229*52*61) nodes and 697680 quadrilateral cells (Fig. 4). The plane z=0 is the plane of symmetry located in the middle of the height of the cylinder.

Histories of residues for both simulations are shown in Fig. 5 (2D) and 6 (3D). The 3D computation time is about 13.5 CPU days using four processors and for 400000 iterations. Both figures indicate that the 2D-3D-**elsA** computations have converged.

Fig. 7 shows the 3D computed profiles of the wall heat-flux along three parallel arcs of a circle on the heated cylinder. The positions x=0 and x=0.084m correspond to the axis of two impacting jets and x=0.042m to the axis of an outlet slot. The profiles for z=-0.0195m and z=0.0195m overlap perfectly, indicating the symmetry of 3D simulations. The comparison (Fig. 8) between the 3D profile in the plane of symmetry and the profile obtained from 2D computations displays very similar shapes.

Flow streamlines obtained from 3D computations are plotted in Fig. 9 in the plane of symmetry (z=0) and the temperature variations are superimposed using a colour map. The flow and temperature patterns look the same as the results of 2D computations presented in Fig. 11. The good agreement between 2D and 3D computations in the vicinity of the plane of symmetry (z=0) leads us to conclude that 2D computations are relevant for further investigations of the FLUENT, **elsA** and Aghora numerical codes.

Errors on the mass flow rates in Tab. 3 and in Tab. 6 are globally less than 0,4% in absolute terms compared to experiment. In Tab. 4 the convective heat transfer is 3.9% better in the case of **elsA**-3D than that of **elsA**-2D compared to experiment. Indeed there is only -1,4% of difference between the **elsA**-3D solution and the experiment against -5,3% when comparing the **elsA**-2D solutions with experiment.
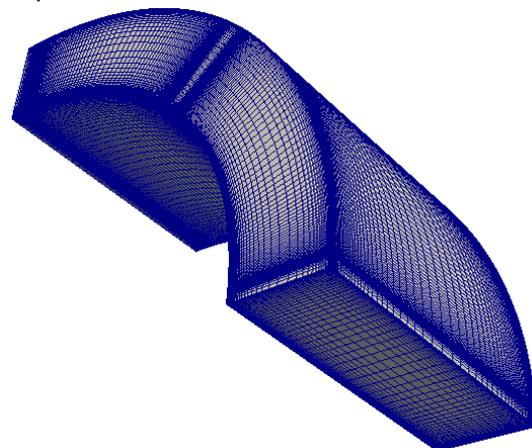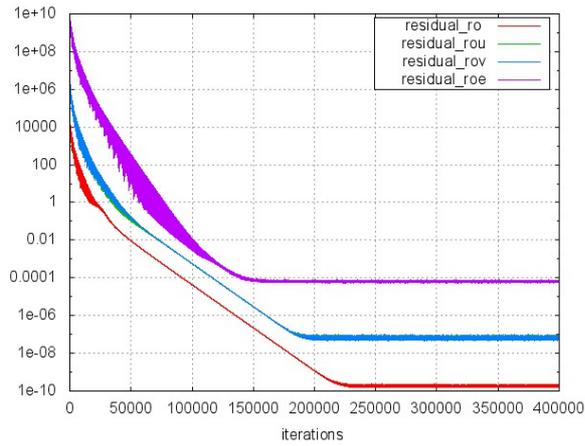

Figure 4: view of the 3D mesh

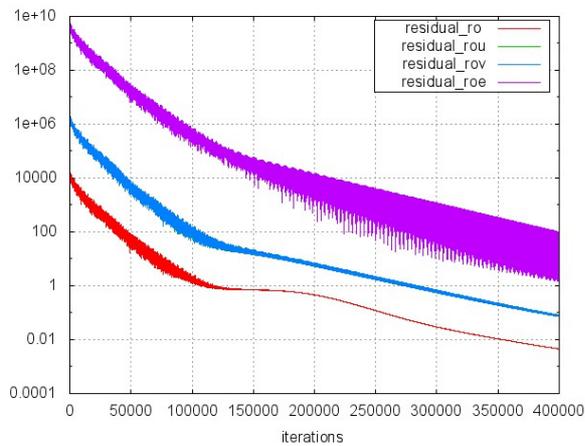*Figure 5: Evolution of residues during 2D computations with **elsA**.*

*Figure 6: Evolution of residues during 3D computation with **elsA**.*
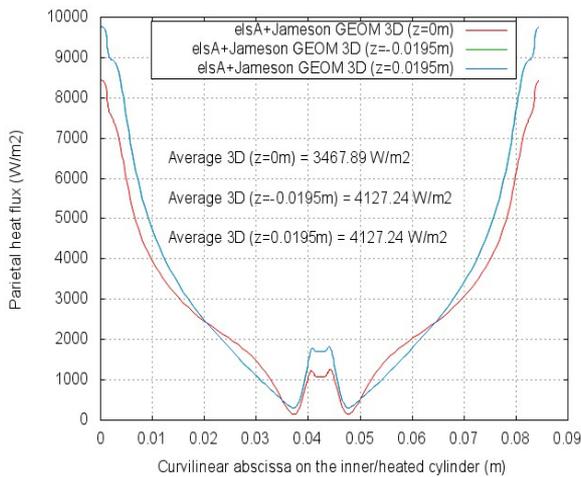

Figure 7: Comparison of heat-fluxes along arcs of circle on the inner-heated cylinder from 3D computations in three different planes.
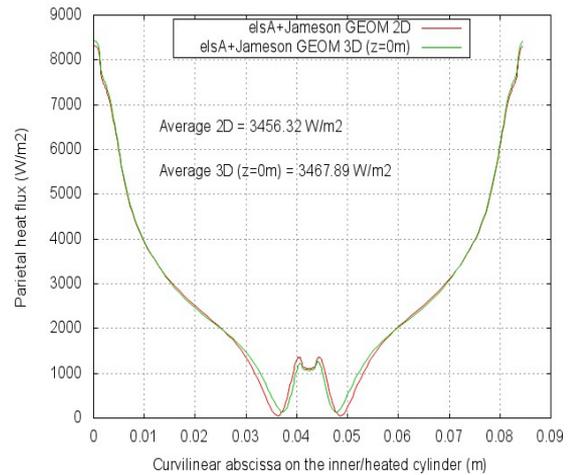

Figure 8: Comparison of heat-fluxes along an arc of circle on the inner-heated cylinder from 2D and 3D computations.
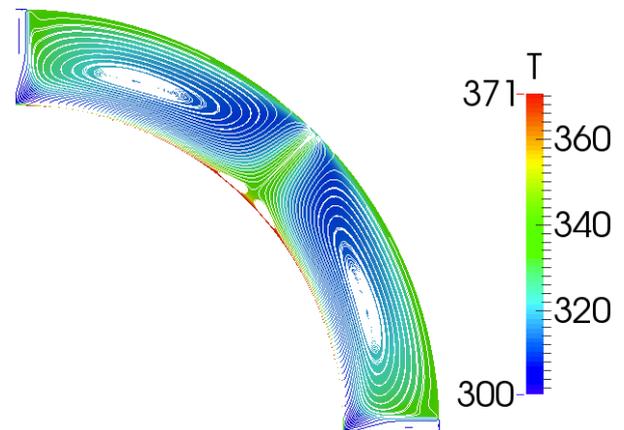

*Figure 9: Flow streamlines superimposed on temperature variations. 3D computations with **elsA**+Jameson 3D. Result in plane z=0m.*

*Table 3. Error on the inlet/outlet mass flow rate with **elsA** 2D and **elsA** 3D.*

	Experience	**elsA** 2D with Jameson	**elsA** 3D with Jameson
Inlet mass flow rate (kg.s^{-1})	0.000888	0.000884	0.000884
Error rate (over the experience)		-0.4 %	-0.4 %
Outlet mass flow rate (kg.s^{-1})	0.000888	0.000886	0.000887
Error rate (outlet over inlet)		0.2 %	0.3 %

Table 4. Convected heat flux comparisons with elsA 2D and elsA 3D. Experience is the reference.

	Experience	**elsA** 2D with Jameson	**elsA** 3D with Jameson
Convected heat flux (W)	20.00	18.93	19.72
Error rate (over the experience)		-5.3 %	-1.4 %

2D-FLUENT-elsA 2D-computations
Technical information on meshes used for the three models are given in Tab. 5. In this paper, the same mesh has been used for all 2D computations.

Fig. 10 to 12 show the streamlines and the temperature fields obtained with ANSYS-Fluent and **elsA**. The main differences are observed in the eddy patterns generated in the annular domain. While the two **elsA** solutions in Fig. 10 and 11 look similar, the Fluent-PISO solution in Fig. 12 displays a more complex eddy pattern. Moreover, although the boundary conditions of the simulation is steady, the FLUENT simulation shows slow spatial oscillations in time. Actually, the FLUENT solution does not converge, whichever the numerical method (SIMPLE or PISO) is used. As a consequence, the outlet mass flow rate and the convective heat flux vary in time. For FLUENT simulations Tab. 6 indicates that the relative error of the mass flow rate between outlet and inlet vary from -1,1% to 0,9% while for **elsA** it is stable of 0,2% for Jameson and of 0,3% for Roe. Tab. 7 indicates also that the convective heat flux for the all computations vary from -25,1% to -5,3% as compared to the experimental value. In that table again, fluctuations and stability of the values are observed respectively with FLUENT and **elsA**.
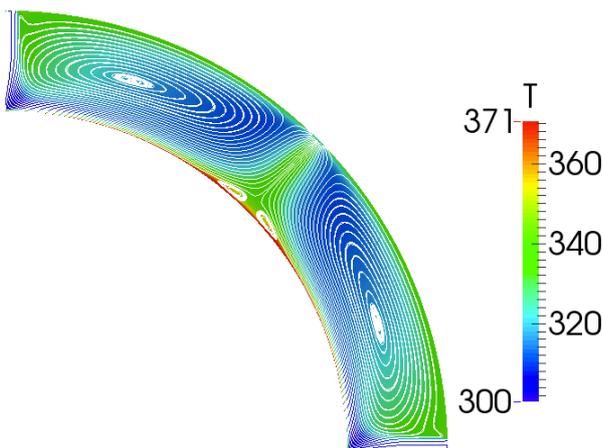

Figure 10: Flow streamlines superimposed on temperature variations. 2D computations with elsA+Jameson

Fig. 13 compares the heat flux along the heated cylinder obtained respectively with ANSYS-Fluent and with the two **elsA** solutions.
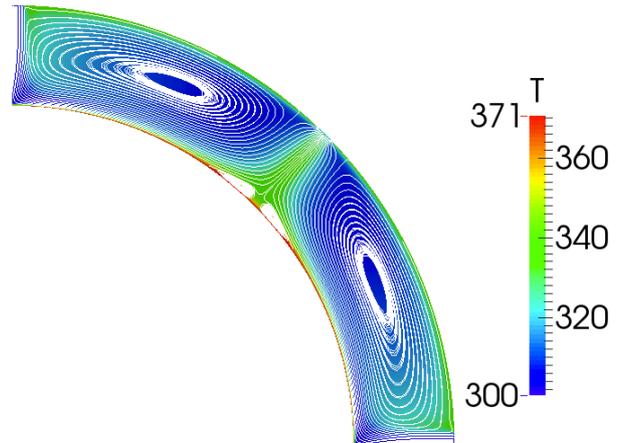

Figure 11: Flow streamlines superimposed on temperature variations. 2D computations with elsA+Roe.
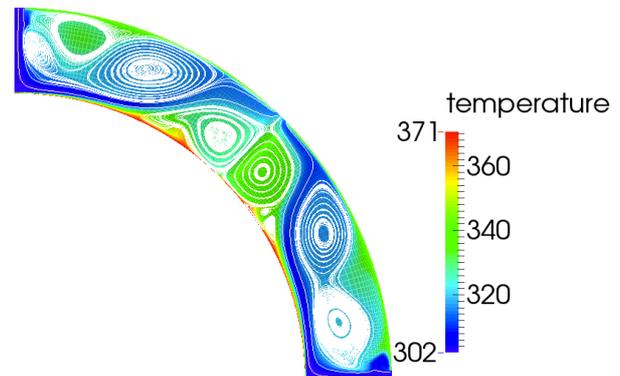

Figure 12: Flow streamlines superimposed on temperature variations. 2D computations with Fluent+PISO (600 000 iters).
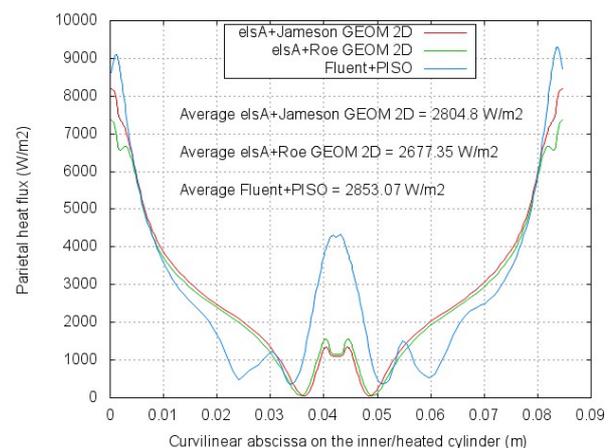

Figure 13: Comparison of heat-fluxes along an arc of circle on the inner-heated cylinder obtained from from 2D computations. with elsA and FLUENT.

*Table 5. Grid breakdown for FLUENT, **elsA** and AGHORA*

	FLUENT, **elsA**, AGHORA
Number of points	11 908
Number of cells	11 628
Cell geometry	Quadrangular
Min and max edge size on the inner-heated cylinder (m)	$6.2e^{-5}$ to $1.1e^{-3}$
Min and max edge size on the outer cylinder (m)	$8.1e^{-5}$ to $1.4e^{-3}$

*Table 6. Error on the inlet/outlet mass flow rate with FLUENT, **elsA**.*

	Experience	*FLUENT with SIMPLE*	*FLUENT with PISO*	***elsA** with Jameson*	***elsA** with Roe*
Inlet mass flow rate ($kg.s^{-1}$)	0.000888	0.000886	0.000886	0.000884	0.000884
Error rate (over the experience)		-0.2 %	-0.2 %	-0.4 %	-0.4 %
Outlet mass flow rate ($kg.s^{-1}$)	0.000888	0.000878 to 0.000896	0.000883 to 0.000892	0.000886	0.000887
Error rate (outlet over inlet)		-1.1% to 0.9%	-0.5% to 0.4%	0.2 %	0.3 %

*Table 7. Convected heat flux comparisons with FLUENT, **elsA**. Experience is the reference.*

	Experience	*FLUENT with SIMPLE*	*FLUENT with PISO*	***elsA** with Jameson*	***elsA** with Roe*
Convected heat flux (W)	20.00	15.17 to 16.48	14.98 to 16.43	18.93	16.85
Error rate (over the experience)		-24.1% to -17.6%	-25.1% to -17.8%	-5.3 %	-15.7 %

2D-Aghora Computations

For this simulation we use a modal approach in which the polynomial degree is set to 1. The order of accuracy of the simulation is therefore 2nd-order. We will denote this simulation DG-p1. The boundary conditions shown in Tab. 8 are those specified for the previous 2D-computations except for the inlet condition. At the inlet boundaries we impose constant values of the total pressure, total temperature, and the direction of the velocity, instead of the mass flow, the total temperature, and the direction of the velocity as is done in the previous 2D-simulations. This choice leads to an inlet mass flow that is smaller than the mass flow imposed in the experiment, and that imposed in the **elsA** and FLUENT computations. This is the reason why we cannot compare the convected heat flux obtained from the DG-p1 simulation with that provided by the experiment.

In this paragraph let us have a look on the comparison between the compressible modelings of Aghora and elsA. It is interesting to look at the temperature field and the streamlines pattern displayed by the DG-p1 simulation (Fig.14), as well as the heat flux profile at the inner wall (Fig. 15). Indeed, from our experience with the **elsA** code, for a given level of artificial dissipation in Jameson scheme, the overall features of the flow are not fundamentally affected by the two different ways of imposing the inlet condition. We can observe from

Fig. 14 the very different behaviour between the results from the **elsA** simulations presented above and that from the DG-p1 simulation.

Table 8. Boundary conditions with AGHORA.

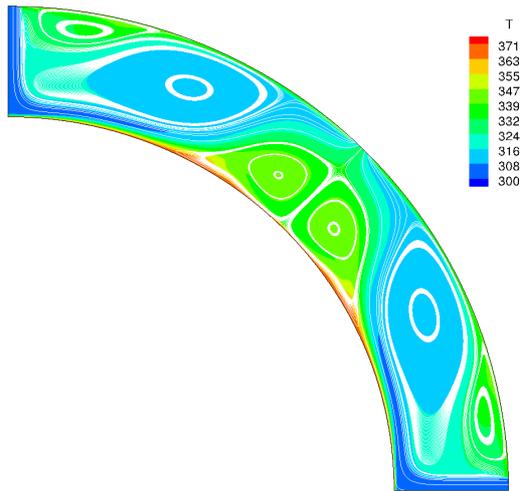|	AGHORA
Inlet	Pressure: 104196.29 Pa Temperature: 302.45 K Velocity direction: (0, -1, 0) or (-1, 0, 0)
Outlet	Pressure: 104 184.83 Pa
Internal wall (heated wall)	Temperature: 370.65 K Temperature: 342.45 K
External wall	

Figure 14: streamlines and temperature field for the DG-p1 simulation using Aghora.

Figure 15: Profile of heat flux at the inner wall along the azimuthal direction. DG-p1 simulation using Aghora.

The main difference lies in the much larger size of the two recirculation bubbles right below the outlet slot, as well as the appearance of two new secondary bubbles near the inlet slots. The authors believe that the reason for the significant differences found is the higher level of artificial dissipation selected in Jameson scheme in the **elsA** computation. Indeed, a number of numerical experiments using **elsA** and Aghora for different values of the artificial viscosity have demonstrated the strong sensitivity of the results to the accuracy of the numerical scheme. The differences in the flow patterns found between the **elsA** and the DG-p1 simulation have a direct effect on the profile of the wall heat-flux as seen from Fig. 15. A comparison with the profiles shown in Fig. 13, highlights the existence of a more intense heat exchange in the vicinity of the outlet axis. As regards the maximum level of heat-flux found in the DG-p1 simulation, it appears to be lower than that found in the other simulations. This is a logical consequence of the lower level of mass flow present in the DG-p1, as mentioned above, which leads to a reduction of the overall heat-exchange in the cooling cavity.

As surprising as it might seem, the result of Aghora as more in common with the result of FLUENT obtained by the incompressible modeling. Indeed comparing the eddy patterns of Figs. 12-14 both have the two recirculation bubbles right below the outlet slot. Moreover looking at Figs 13-15, the behaviours of the wall heat-flux looks the same even if the levels are different.
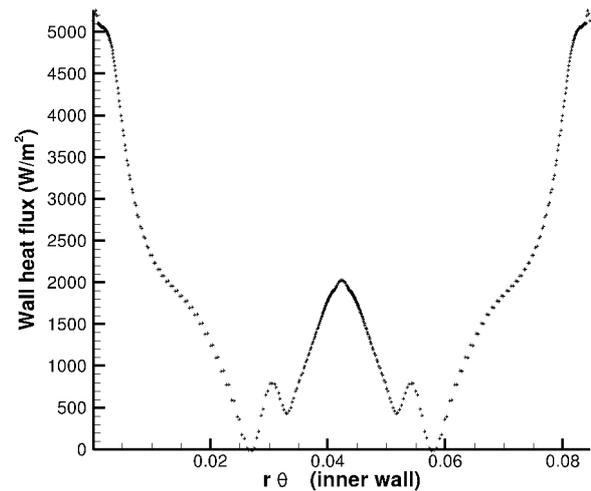
5. CONCLUSION AND PERSPECTIVES

In the context of onboard green aircraft projects, the increasing use of electrical engines requires more efficient cooling systems. This study presents the results of a comparative study of simulations by various incompressible or compressible CFD models of the convective heat transfer achieved by impacting jets. The test case is given by a specific laboratory experiment, which is devoted at the university of Pau to the study of cooling of small-sized turbo engines.

Comparisons between the results from 3D and 2D computations support the relevance of 2D models for simulating the convective heat transfer by the impacting jets as carried out in the experiment.

The present study focuses on low Reynolds number confined flow conditions. A comparison is made between the results of numerical simulations obtained using incompressible models of FLUENT and the compressible ones of **elsA** and Aghora. The flow fields obtained by the three codes show eddy patterns in the annular domain simulated, which differ in detail.

Even though the boundary conditions are steady, the results obtained with the incompressible models of FLUENT display instabilities while the compressible models of **elsA** are stable with residuals which seem to converge. Thus the parietal heat-flux distributions along the inner wall, predicted by the different models, display differences. Nevertheless, the average of these fluxes are the same within less than 2%. For flow conditions the global convective heat fluxes computed with FLUENT and **elsA** are ranging from 0.75 to 0.95 of the experimental data. In such a CFD case, the stability of the fluid seems to be a key issue linked with the compressibility effects.

A second-order DG simulation has also been performed with a lower inlet mass rate using the Aghora compressible solver, by setting the polynomial degree to 1 (DG-p1) and using the same mesh resolution as in previous 2D-simulations. The solutions from the two compressible solvers (i.e. *elsA* and Aghora) appear to be fundamentally different. Concerning the Jameson scheme, the authors believe that the reason for the significant difference founds is the higher level of artificial dissipation selected in Jameson scheme in the *elsA* computations. This has a direct effect on the profile of the wall heat-flux, for which the existence of a more intense heat exchange in the vicinity of the outlet axis is observed in the case of the DG-p1 simulation. As the inlet mass flow rate is slightly lower compared to those used in *elsA* and FLUENT it not surprising that the level of the wall heat-flux is also lower. However its behaviour as the eddy pattern look rather the same than that provided by the incompressible modeling with FLUENT.

A new boundary condition with imposition of the mass flow is being implemented in the Aghora solver and new simulations are planned in order to verify the conclusions from this preliminary analysis. It would also be of great interest to perform higher-order simulations using Aghora (at least p=2 and p=3). Indeed, one of the remarkable properties of high-order methods is the little influence of the selected numerical flux (convective and viscous) on the accuracy of the solution.

It is encouraging that the results of simulations are in qualitative agreement with the laboratory experiments and recover the order of magnitude of the total heat transfer measured. Nevertheless, much remain to be done. Modeling compressible fluid flows is known to be difficult for low Mach number conditions. Our goal is orient ourselves into the development of "All Mach" solvers.

REFERENCES

[1]. Franklyn J. Kelecy. Coupling momentum and continuity increases CFD robustness, ANSYS advantage, volume II, issue 2, 2008.

[2]. L. Cambier, S. Heib, and S. Plot. The ONERA *elsA* CFD software : input from research and feedback from industry. *Mechanics & Industry*, 14(03), pp.159–174, 2013.

[3]. M. de la Llave Plata, V. Couaillier, C. Marmignon, M.C. Le Pape, M. Gazaix, B. Cantaloube, "Further developments in the multiblock hybrid CFD solver elsA-H", AIAA paper 2012-1112

[4]. P. L. Roe. Approximate Riemann Solvers, Parameter Vectors, and Difference Schemes. J. Comput. Phys., 43:357–372, 1981.

[5]. A. Jameson, W. Schmidt, and E. Turkel. Numerical Solution of the Euler Equations by Finite Volume Methods using Runge–Kutta Stepping Schemes. Technical Report 81–1259, AIAA, 1981.

[6]. F. Renac, M. de la Llave Plata, E. Martin, J.-B. Chapelier, and V. Couaillier, Aghora : A High-Order DG Solver for Turbulent Flow Simulations. IDIHOM : Industrialization of High-Order Methods - A Top-Down Approach, Notes on Numerical Fluid Mechanics and Multidisciplinary Design, N. Kroll, C. Hirsch, F. Bassi, C. Johnston, and K. Hillewaert, 128 (2014) pp. 315-335, Springer.

[7]. J.-B. Chapelier, M. de la Llave Plata, F. Renac, and E. Lamballais. Eva- luation of a high-order discontinuous Galerkin method for the DNS of turbulent flows. Comput. Fluids, 95 (2014), pp. 210-226

[8]. F. Bassi, S. Rebay, G. Mariotti, S. Pedinotti and M. Savini, A High-order accurate discontinuous finite element method for inviscid and viscous turbomachinery Flows, In proceedings of the 2nd European Conference on Turbomachinery Fluid Dynamics and Thermodynamics, R. Decuypere, G. Dibelius (eds.), Antwerpen, Belgium, 1997.

[9]. R. Hartmann and P. Houston, An optimal order interior penalty discontinuous Galerkin discretization of the compressible Navier-Stokes equations J. Comput. Phys. 227 (2008), pp. 9670-9685.

[10]. R. J. Spiteri and S. J. Ruuth, A new class of optimal high-order strong stability preserving time discretization methods, SIAM J. Numer. Anal., 40 (2002), pp. 469-491.